Accepted Manuscript

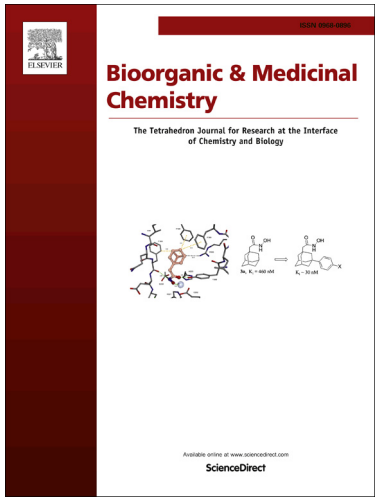

Design, synthesis and preliminary biological evaluation of indoline-2,3-dione derivatives as novel HDAC inhibitors

Kang Jin, Shanshan Li, Xiaoguang Li, Jian Zhang, Wenfang Xu, Xuechen Li

PII: S0968-0896(15)00470-8
DOI: http://dx.doi.org/10.1016/j.bmc.2015.05.048
Reference: BMC 12344

To appear in: *Bioorganic & Medicinal Chemistry*

Received Date: 3 March 2015
Revised Date: 26 May 2015
Accepted Date: 27 May 2015

Please cite this article as: Jin, K., Li, S., Li, X., Zhang, J., Xu, W., Li, X., Design, synthesis and preliminary biological evaluation of indoline-2,3-dione derivatives as novel HDAC inhibitors, *Bioorganic & Medicinal Chemistry* (2015), doi: http://dx.doi.org/10.1016/j.bmc.2015.05.048

Design, synthesis and preliminary biological evaluation of indoline-2,3-dione derivatives as novel HDAC inhibitors

Kang Jin[a], Shanshan Li[a], Xiaoguang Li[a], Jian Zhang[a],Wenfang Xu[a*,†], and Xuechen Li[b,*,†]

[a] *Department of Medicinal Chemistry, School of Pharmacy, Shandong University, Jinan, Shandong 250012, China*

[b] *Department of Chemistry, The University of Hong Kong Pokfulam Road, Hong Kong (P.R. China)*

** Corresponding author.*

† These authors contributed equally.

Abstract

Histone deacetylases (HDACs) are Zinc-dependent or NAD^+ dependent enzymes and play a critical role in the process of tumor development. Herein a series of indoline-2,3-dione derivatives have been designed and synthesized as potential HDACs inhibitors. The preliminary biological evaluation showed that most compounds synthesized have exhibited moderate Hela cell nuclear extract inhibitory activities, among which compound **25a** (IC_{50}= 10.13 nM) has shown the best efficacy. The anti-proliferative activities of some of these compounds were also discussed.

Keywords: Indoline-2,3-dione derivatives; HDAC inhibitors; Synthesis; Biological evaluation; QSAR

*Corresponding Author: Wenfang Xu
Department of Medicinal Chemistry, School of Pharmaceutical Sciences, Shandong University 44, West Culture Road, Jinan 250012, P. R. China
TEL +86-531-88382264; fax: +86 531 88382264; E-mail: wfxu@yahoo.cn(W. Xu).

*Corresponding Author: Xuechen Li
Department of Chemistry, The University of Hong Kong Pokfulam Road, Hong Kong (P.R. China)
TEL: (852) 2219 4992; E-mail: xuechenl@hku.hk.

1. Introduction

Cancer has long been known as the most tortuous and life-threatening disease in the world. Every year, tens of thousands of people lose their lives due to the lack of effective treatments, especially the effective anti-tumor drugs. In recent years, a great many of relevant anti-cancer targets, such as the histone deacetylases (HDACs), have been reported.

Histone deacetylases (HDACs), as Zinc-dependent or NAD^+ dependent enzymes, are responsible for the deacetylation of lysine residues located in various protein substrates, such as nucleosomal histones[1]. As a result of the deacetylation, the increased positive charge density on the N-termini of nucleosomal histones can strengthen the binding to the negatively charged chromosomal DNA, resulting in the repression of the genetic transcription[2-4]. In this way, HDACs play a critical role in remodeling chromatin and down-regulating many genes expression. In addition, many other non-histone proteins have also been reported as HDACs substrates recently, such as molecular chaperones, cytoskeletal proteins, transcription factors and nuclear import factors, which are related to the survival pathways and cell growth[5]. The hypo-acetylation of many histones and non-histone proteins has been known to be associated with many pathogenic mechanisms, especially carcinogenesis[6].

HDACs in the human can be categorized into four classes. Class Ⅰ (HDACs 1-3 and 8), Ⅱ (HDACs 4-7,9 and 10) and Ⅳ (HDACs 11) are Zinc-dependent enzymes, while the class Ⅲ HDACs (sirtuins 1–7) are NAD^+ dependent[7]. It has been shown that the dysregulation of class I and Ⅱ HDACs, especially class I isozymes, has been linked to the process of tumor cells proliferation, angiogenesis, invasion and metastasis[8-15]. Over the past few years, numerous novel and efficient HDAC inhibitors (HDACi) have been reported as potential antitumor agents, among which, SAHA (Zolinza®, Merck, Fig. 1)[16] and FK228 (Istodax®, Gloucester Phar-maceuticals/Celgene, Fig. 1)[17], have already been on the market.

As we can see in the **Figure 1**, a powerful HDACi generally contains three

domains: a zinc binding group (ZBG), a hydrophobic cap group and a linker in a certain length connecting the ZBG and a cap group[1]. According to the previous work in our group, compound **10c** is excellent APN inhibitor, which also possesses similar structural characteristic as the HDAC inhibitors. Hence, we wished to design and synthesize a series of novel indoline-2,3-dione derivatives (**Fig. 2**) as potential HDACs inhibitors in order to search for more valuable candidates for the tumor therapy. In this report, the synthesis, biological evaluation and docking studies of these compounds were discussed.

2. Chemistry

The target compounds were all synthesized by taking advantage of some commonly used chemical reagents in the laboratory. As shown in the **scheme 1**, the crucial intermediate **3** was synthesized through the Sandmeyer reaction using 4-bromoaniline. Compound **2**, prepared from the reaction of **1**, hydroxylamine hydrochloride and chloral hydrate, could be converted to **3** with concentrated sulfuric acid at 90℃. Compound **4** could be obtained by the reaction between methyl **3** and ethane-1,2-diol, which was then coupled with methyl 2-bromoacetate to produce compound **5**. After the hydrolysis of methyl ester, the condensation between amino acid methyl esters of different lengths with the carboxylic acid group of compound **6** proceeded to afford **7a-7d**. The target compounds **8a-8d** were obtained by the treatment of **7a-7d** with NH_2OK in methanol.

The target compounds **16a-16e** were synthesized follwoing the same sequence as **7a-7d** by using different substituted anilines as the starting material, as shown in **scheme 2**. Compounds **11b-11c** were coupled with propane-1,3-diol or butane-1,4-diol under acidic environment to give rise to **17a-17d**. Following the procedure noted before, target compounds **21a-21d** were thus prepared (**scheme 3**). In addition, the intermediate **17c** could react with methyl 3-bromopropanoate or methyl 4-bromobutanoate to give **22a-22b**, which then could be used to synthesize other two target compounds **25a-25b** just as the steps provided before (**scheme 4**).

Finally, compound **27** was obtained by the condensation of benzene-1,2-diamine and **26** which was derived from hydrolysis of **20c** (**scheme 5**).

3. Results and discussion

All the target compounds were tested using HeLa cell nuclear extract (which mainly contains HDAC1 and HDAC2) as the enzyme source and the results were listed in **Table 1** to **Table 5**. As the data shown in **Table 1** and **Table 2**, different lengths of the side chain would lead to the different HDACs inhibitory activities. Compared with compounds **8a-d**, compound **16c** displayed a better potency, which indicated that the length of this side chain was much more suitable for using in HDACs inhibitors.

In order to explore the effect of different substituents in $\mathbf{R_1}$ position, compounds **16a-f** were synthesized and assayed for their potential HDACs inhibitory activities. From the data of **Table 2**, compound **16c** with a bromide group on the benzene ring exhibited the most powerful inhibitory activity. This may be due to the fact that the negative inductive effect of bromide is weaker than fluorine and chlorine, so that the π-electron density on the benzene ring is a little denser. Thus, the π-π interaction between benzene and the residues in the rim of the HDACs active site is slightly stronger. This also explained why compound **16f** with a nitrogroup in $\mathbf{R_1}$ position had an extremely poorer activity compared to the other compounds in **Table 2**. In addition, the activity of compound **16c** is better than compound **16d** and **16e**, which may be related to the size of group $\mathbf{R_1}$ and the steric hindrance effect between $\mathbf{R_1}$ and the active site of HDACs, and bromine atom is much more applicable to be used in the further development of HDACs inhibitors in this experiment.

The compounds in **Table 3** were specifically designed to investigate the effect of ketal spiro rings at the 3-postion of indolin-2-one skeleton. The data in **Table 3** showed that compounds **21a-b** and **21c-d** exhibited better activities than **16b** and **16c** respectively. It is likely that the enlargement of heterocycle had influenced the steric hindrance and enhanced the ability to form the hydrophobic effect. Otherwise, 6-membered heterocyclic derivatives **21a** and **21c** displayed a higher potency for the inhibition of HDACs than 7-membered heterocyclic counterparts **21b** and **21d** respectively. This may be explained by that the

6-membered heterocyclic ring is more stable and suitable for the hydrophobic effect than 7-membered ones.

After the effect of the substituent in $\mathbf{R_1}$ and the size of heterocyclic ring have been determined, two compounds with longer side chains have been synthesized (**Table 4**). Compared with **21c**, compounds **25a** exhibited a better inhibitory activity but the inhibitory potency of **25b** was a little lower. This showed that the length of the side chain of compound **25a** was fitted better to occupy the active site of HDACs.

Compounds in **Table 5** were synthesized to study the effect of hydroximic acid. From the data, we could see that compounds **20c** and **26** showed very weak inhibitory potency. Although **27** was more potent, it was still not as good as **21c** and contrast **SAHA**. This means that hydroximic acid had stronger zinc-chelating activity than o-phenylenediamine, hydroxyl and methoxyl groups. And it could bind to the active site of HDACs much more solidly.

To further assay the anti-tumor inhibitory activity of these derivatives, several potent compounds were selected to test their antiproliferative effects on twelve common tumor cell lines with SAHA as the positive control. The result showed in **Table 6** suggested that compound **25a** showed stronger inhibitory ability than other inhibitors against most tumor lines, especially several suspension cell lines such as K562 cell (chronic myeloid leukemia, CML), U937 cell (histiocytic lymphoma), HEL cell (leukemia cell line) and KG1 cell (leukemia cell line). In addition, other solid tumor cells were also very sensitive to our compounds except for MDA-MB-231 cell (breast cancer). Based on this information, a subcutaneous H7402 xenograft model was established. Once the volume of tumors became about 140mm^3, mice were dosed with compound **25a** or **SAHA** for 16 days. The gavage administration of compound **25a** and **SAHA** were at different dosages, 60mg/kg/d and 100mg/kg/d separately. During the treatment, no significant body weight variation and toxicity were detected. The relative increment ratio (T/C) of **25a** was 62.50%, meanwhile **SAHA** was 75.53%. Both the SAHA-treated group and the 25a-treated group were significantly

different from the control group ($p < 0.05$) by two-tailed t test. As the result shown in **Figure 3**, the in vivo antitumor efficacy of compound **25a** (60mg/kg/d) was a little better than that of **SAHA** (100mg/kg/d). Since the dosage of **25a** was far less than that of **SAHA**, the potency of **25a** was much higher compared to that of **SAHA**.

Aiming to investigate the HDAC isoform selectivity of the indoline-2,3-dione derivatives, we selected compound **25a** to assay enzyme inhibition against HDAC1, HDAC3 and HDAC6. The results (**Table 7**) confirmed that our indoline-2,3-dione inhibitors exhibited well selectivity against individual HDACs.

In order to investigate the interaction between target compounds and HDACs, we selected compound **25a** to dock into the active site of HDAC8 (PDB entry: 1T64) using a sybyl/Sketch module and optimized via Powell's method by the Tripos force field with convergence criterion set at 0.05 kcal/(Å mol), and assigned with the Gasteiger-Hückel method. The docking study of **25a** and the active site of HDAC8 was performed using Sybyl/FlexX module. The active site was defined as 8.0 Å radius circles around TSA in the co-crystal structure (PDB entry: 1T64). Other docking parameters utilized in the program were kept default. As the result shown in **Figure 4**, hydroxamic acid group can form a chelated structure with the zinc ion in the centre of active site and the side chain can occupy the long and narrow passage which links the zinc and the outside world. To obtain the detailed binding mode, a 2D pattern was created as well (**Figure 5**), which suggested that the isatin structure of compound **25a** can form hydrophobic interaction with Gly^{206} and Phe^{207} around the opening of the passage.

4. Conclusion

Based on the previous work in our laboratory, a series of indoline-2,3-dione derivates were designed and synthesized as HDAC inhibitors. Among them, most compounds exhibited potent activities in the in vitro HDAC inhibition assay and antiproliferative assay. Especially, the compounds **21c**, **25a** and **25b** showed low-nanomolar IC_{50} values. Compound **25a** was also evaluated for the in vivo antitumor assay in a H7402 xenograft mice model, and exhibited more potent efficacy than that of approved drug **SAHA**. Further structure transformation of **25a** for more effective HDAC inhibitors is underway in our laboratory.

5. Experiment

5.1. Chemistry: general procedures

All the starting reactants, solvents, and catalysts were commercially available unless otherwise stated. All solvents, except for those aqueous media, were purified by standard techniques in order to exclude the moisture. All reactions were monitored by thin-layer chromatography with 0.25 mm silica gel plates (60GF-254). The spots were visualized with UV light, iodine vapor or ferric chloride. ^{1}H NMR spectra were determined on a Brucker DRX spectrometer at 600 MHz for 1H, δin parts per million (ppm) and *J* in Hertz. ESI-MS were recorded on an API 4000 spectrometer, and HRMS were conducted by Shandong Analysis and Test Center in Ji'nan, China. Melting points were recorded using an uncorrected electrothermal melting point apparatus. Parts of targeted products were analysed by HPLC on an Agilent 1100 HPLC instrument using a Phenomenex Synergi 4μ Hydro-RP 80A column (250 mm ×4.6 mm) through one of the following methods. Method A: compounds **21a**, **21b**, **25a** were eluted with 50% methanol/50% water (containing 0.1% formic acid) over 15 min, with a flow rate of 2.0 mL/min and detection at 267 nm. Method B: compounds **25b** were eluted with 55% methanol/45% water (containing 0.1% formic acid) over 15 min, with a flow rate of 2.0 mL/min and detection at 267 nm. Method C: compounds **27** were eluted with 65% methanol/35% water (containing 0.1% formic acid) over 10 min, with a flow rate of 2.0 mL/min and detection at 267 nm.

N-(4-bromophenyl)-2-(hydroxyimino) acetamide (**2**), 5-bromoindoline-2,3-dione (**3**), 5'-bromospiro[[1,3]dioxolane-2,3'-indolin]-2'-one (**4**), Methyl-2-(5'-bromo-2'- oxospiro[[1,3]dioxolane-2,3'-indoline]-1'-yl)acetate (**5**), 2-(5'-bromo-2'-oxospiro [[1,3]dioxolane-2,3'-indoline]-1'-yl)-N-(2-(hydroxyamino)-2-oxoethyl)aceta

mide (**7a**), 2-(5'-fluoro-2'-oxospiro[[1,3]dioxolane-2,3'-indoline]-1'-yl)acetic acid (**14a**) and its analogues**14b-f**, methyl-2-(5'-chloro-2'-oxospiro[[1,3]dioxane-2,3'-indoline] -1'-yl)acetate (**18a**) and its analogues **18c-d**, were prepared based on the procedures described previously[18].

General procedure for the preparation of 8a and its Analogue 8b-d.

5.1.1. 2-(5'-bromo-2'-oxospiro[[1,3]dioxolane-2,3'-indoline]-1'-yl)-N-(2-(hydroxyamino)-2-oxoethyl)acetamide (8a).

To a solution of 1.5 N NH_2-OK in methanol (10mL) was compound **7a** (0.5 g, 1.25 mmol) added. The mixture was stirred at room temperature for about 1.5 h and then concentrated in vacuum. The residue was dissolved in 50mL EtOAc. 1N HCl was added to the solution while shaking the container until the PH of aqueous layer became weakly basic. The organic layer was separated using a separatory funnel, dried with Na_2SO_4, and then evaporated under low pressure to obtain the crude product. Finally, the crude product was purified by column chromatography (P/E=1:1) to get compound **8a** as white solid (0.26 g, 52.0% yield). mp=176-177℃. .^{1}H NMR (600 MHz, DMSO) δ 10.57 (s, 1H), 8.86 (d, J = 1.3 Hz, 1H), 8.57 (t, J = 5.8 Hz, 1H), 7.61 – 7.56 (m, 2H), 6.92 – 6.90 (m, 1H), 4.35 – 4.32 (m, 4H), 4.32 – 4.30 (m, 2H), 3.65 (d, J = 5.8 Hz, 2H). HRMS (AP-ESI) m/z Calcd for $C_{14}H_{14}BrN_3O_6$ [M+H]+ 400.0066, found 400.0141.

5.1.2. 4-(2-(5'-bromo-2'-oxospiro[[1,3]dioxolane-2,3'-indoline]-1'-yl)acetamido)-N-hydroxybutanamide (8b).

White solid, yield 41.3%. mp=159-160℃. ^{1}H NMR (600 MHz, DMSO) δ 10.36 (s, 1H), 8.70 (s, 1H), 8.27 (t, *J* = 5.5 Hz, 1H), 7.60 (dd, *J* = 6.8, 2.0 Hz, 2H), 6.90 – 6.87 (m, 1H), 4.33 (dd, *J* = 4.1, 2.7 Hz, 2H), 4.32 – 4.30 (m, 2H), 4.25 (s, 2H), 3.05 (dd, *J* = 12.9, 6.7 Hz, 2H), 1.96 (t, *J* = 7.5 Hz, 2H), 1.66 – 1.60 (m, 2H). HRMS (AP-ESI) m/z Calcd for $C_{16}H_{18}BrN_3O_6$ [M+H]+ 428.0379, found 428.0447.

5.1.3. 6-(2-(5'-bromo-2'-oxospiro[[1,3]dioxolane-2,3'-indoline]-1'-yl)acetamido) -N-hydroxyhexanamide (8c).

White solid, yield 57.4%. mp=158-159℃. ^{1}H NMR (600 MHz, DMSO) δ 10.34 (s, 1H), 8.67 (s, 1H), 8.23 (t, *J* = 5.5 Hz, 1H), 7.62 – 7.58 (m, 2H), 6.87 (d, *J* = 8.3 Hz, 1H), 4.34 – 4.32 (m, 2H), 4.32 – 4.30 (m, 2H), 4.24 (s, 2H), 3.05 (dd, *J* = 12.7, 6.7 Hz, 2H), 1.94 (t, *J* = 7.4 Hz, 2H), 1.51 – 1.44 (m, 2H), 1.40 (dt, *J* = 14.6, 7.1 Hz, 2H), 1.27 – 1.20 (m, 2H). HRMS (AP-ESI) m/z Calcd for $C_{18}H_{22}BrN_3O_6$ [M+H]+ 456.0692, found 456.0766.

5.1.4. (E)-3-(4-(2-(5'-bromo-2'-oxospiro[[1,3]dioxolane-2,3'-indoline]-1'-yl)acet amido)phenyl)-N-hydroxyacrylamide (8d).

White solid, yield 53.2%. mp=223-224℃. ^{1}H NMR (600 MHz, DMSO) δ 10.71 (s, 1H), 10.19 (s, 1H), 9.00 (s, 1H), 7.64 (d, *J* = 8.4 Hz, 2H), 7.52 (d, *J* = 8.3 Hz, 2H), 7.45 (d, *J* = 2.4 Hz, 1H), 7.40 (d, *J* = 15.7 Hz, 1H), 7.36 (dd, *J* = 8.7, 2.4 Hz, 1H), 6.49 (d, *J* = 8.8 Hz, 1H), 6.37 (d, *J* = 15.8 Hz, 1H), 4.17 (t, *J* = 6.8 Hz, 2H), 4.07 (t, *J* = 6.9 Hz, 2H), 3.94 (s, 2H). HRMS (AP-ESI) m/z Calcd for $C_{21}H_{18}BrN_3O_6$ [M+H]+ 488.0379, found 488.0423.

5.1.5. Methyl4-(2-(5'-fluoro-2'-oxospiro[[1,3]dioxolane-2,3'-indoline]-1'-yl)acet amido)benzoate(15a)

A solution of compound **14a** (0.50 g, 1.87 mmol) in 30ml anhydrous THF was prepared, then N-methylmorpholine (0.25 mL, 2.24 mmol) and isobutyl chloroformate (0.29 mL, 2.24 mmol) were added successively at -15℃. The reaction was kept at the same temperature for 30 min. And a solution of compound 4-Amino-benzoic acid methyl ester (0.31 g, 2.06 mmol) in 20mL THF was added dropwise to the mixture. 1 h later, the cooling bath was moved away, and the mixture was stirred at room temperature for anothre 20 h. THF was evaporated in vacuum with the residue being dissolved in 50mL EtOAc. The EtOAc solution was washed with saturated citric acid, saturated $NaHCO_3$ and brine in turn, dried over Na_2SO_4, and concentrated with a rotary evaporator to obtain crude product. Finally, the

crude product was purified by column chromatography (P/E=5:1) to get compound **15a** as white solid (0.60 g, 80.2% yield).

Compounds **15b-f** were synthesized by the same method.

5.1.6. Methyl-4-(2-(5'-chloro-2'-oxospiro[[1,3]dioxolane-2,3'-indoline]-1'-yl)acetamido)benzoate (15b).

White solid, 82.1% yield.

5.1.7. Methyl-4-(2-(5'-bromo-2'-oxospiro[[1,3]dioxolane-2,3'-indoline]-1'-yl)acetamido)benzoate (15c).

White solid, 79.6% yield.

5.1.8. Methyl-4-(2-(2'-oxospiro[[1,3]dioxolane-2,3'-indoline]-1'-yl)acetamido)benzoate (15d).

White solid, 81.4% yield.

5.1.9. Methyl-4-(2-(5'-methyl-2'-oxospiro[[1,3]dioxolane-2,3'-indoline]-1'-yl)acetamido)benzoate (15e).

White solid, 82.5% yield.

5.1.10. Methyl-4-(2-(5'-nitro-2'-oxospiro[[1,3]dioxolane-2,3'-indoline]-1'-yl)acetamido)benzoate (15f)

White solid, 76.3% yield.

Compounds **16a-f** were synthesized by the same method as compound **8a**.

General procedure for the preparation of 16a and its Analogue 16b-f.

5.1.11. 4-(2-(5'-fluoro-2'-oxospiro[[1,3]dioxolane-2,3'-indoline]-1'-yl)acetamido)-N-hydroxybenzamide (16a).

White solid, yield 46.2%. mp=248-249℃. ^{1}H NMR (600 MHz, DMSO) δ 11.12 (s, 1H), 10.72 (s, 1H), 10.63 (s, 1H), 7.90 (d, *J* = 8.8 Hz, 1H), 7.70 (dd, *J* = 22.7, 8.8 Hz, 2H), 7.63 (d, *J* = 8.8 Hz, 1H), 7.36 (dd, *J* = 7.6, 2.8 Hz, 1H), 7.27 (td, *J* = 9.1, 2.7 Hz, 1H), 7.09 – 7.05 (m, 1H), 4.55 (d, *J* = 8.7 Hz, 2H), 4.36 (dd, *J* = 4.6, 2.7 Hz, 2H), 4.32 (dd, *J* = 4.7, 2.6 Hz, 2H). HRMS (AP-ESI) m/z Calcd for $C_{19}H_{16}FN_3O_6$ [M+H]+ 402.1023, found 402.1091.

5.1.12. 4-(2-(5'-chloro-2'-oxospiro[[1,3]dioxolane-2,3'-indoline]-1'-yl)acetamido) -N-hydroxybenzamide (16b).

White solid, yield 43.9%. mp=201-202℃. ^{1}H NMR (600 MHz, DMSO) δ 11.12 (s, 1H), 10.70 (s, 1H), 10.61 (s, 1H), 7.90 (d, *J* = 8.8 Hz, 1H), 7.72 (d, *J* = 8.8 Hz, 1H), 7.68 (d, *J* = 8.8 Hz, 1H), 7.62 (d, *J* = 8.8 Hz, 1H), 7.52 (dd, *J* = 4.3, 2.2 Hz, 1H), 7.49 (dd, *J* = 8.4, 1.9 Hz, 1H), 7.10 (dd, *J* = 8.4, 5.6 Hz, 1H), 4.56 (d, *J* = 8.6 Hz, 2H), 4.35 (dd, *J* = 4.2, 2.8 Hz, 2H), 4.33 (d, *J* = 3.7 Hz, 2H). HRMS (AP-ESI) m/z Calcd for $C_{19}H_{16}ClN_3O_6$ [M+H]+ 418.0728, found 418.0796.

5.1.13. 4-(2-(5'-bromo-2'-oxospiro[[1,3]dioxolane-2,3'-indoline]-1'-yl)acetamido) -N-hydroxybenzamide (16c).

White solid, yield 54.3%. mp=263-264℃. ^{1}H NMR (600 MHz, DMSO) δ 11.12 (s, 1H), 10.62 (s, 1H), 8.95 (s, 1H), 7.72 (d, *J* = 8.5 Hz, 2H), 7.63 (dd, *J* = 20.6, 8.2 Hz, 4H), 7.04 (d, *J* = 8.1 Hz, 1H), 4.54 (s, 2H), 4.34 (d, *J* = 5.3 Hz, 4H). HRMS (AP-ESI) m/z Calcd for $C_{19}H_{16}BrN_3O_6$ [M+H]+ 462.0222, found 462.0268.

5.1.14. N-hydroxy-4-(2-(2'-oxospiro[[1,3]dioxolane-2,3'-indoline]-1'-yl)acetamid o)benzamide (16d).

White solid, yield 54.3%. mp=184-185℃. ^{1}H NMR (600 MHz, DMSO) δ 11.12 (s, 1H), 10.72 (s, 1H), 10.62 (s, 1H), 7.90 (d, *J* = 8.8 Hz, 1H), 7.72 (d, *J* = 8.8 Hz, 1H), 7.69 (d, *J* = 8.8 Hz, 1H), 7.63 (d, *J* = 8.8 Hz, 1H), 7.43 – 7.38 (m, 2H), 7.10 (t, *J* = 7.5 Hz, 1H), 7.03 (dd, *J* = 8.4, 4.7 Hz, 1H), 4.54 (d, *J* = 8.9 Hz, 2H), 4.39 – 4.36 (m, 2H), 4.31 (dd, *J* = 4.5, 2.3 Hz, 2H). HRMS (AP-ESI) m/z Calcd for $C_{19}H_{17}N_3O_6$ [M+H]+ 384.1117, found 384.1187.

5.1.15. N-hydroxy-4-(2-(5'-methyl-2'-oxospiro[[1,3]dioxolane-2,3'-indoline]-1'-yl)acetamido)benzamide (16e).

White solid, yield 48.7%. mp=194-195℃. ^{1}H NMR (600 MHz, DMSO) δ 11.12 (s, 1H), 10.69 (s, 1H), 10.60 (s, 1H), 7.90 (d, *J* = 8.8 Hz, 1H), 7.72 (d, *J* = 8.8 Hz, 1H), 7.70 – 7.67 (m, 1H), 7.63 (d, *J* = 8.8 Hz, 1H), 7.24 – 7.18 (m, 2H), 6.91 (dd, *J* = 8.0, 5.1 Hz, 1H), 4.51 (d, *J* = 8.9 Hz, 2H), 4.36 (dd, *J* = 4.0,

2.4 Hz, 2H), 4.30 – 4.28 (m, 2H), 2.28 (s, 3H). HRMS (AP-ESI) m/z Calcd for $C_{20}H_{19}N_3O_6$ [M+H]+ 398.1274, found 398.1333.

5.1.16. N-hydroxy-4-(2-(5'-nitro-2'-oxospiro[[1,3]dioxolane-2,3'-indoline]-1'-yl)acetamido)benzamide (16f).

White solid, yield 41.5%. mp=136-137℃. ^{1}H NMR (600 MHz, DMSO) δ 11.21 (s, 1H), 10.81 (s, 1H), 10.13 (s, 1H), 8.24 (d, *J* = 2.8 Hz, 1H), 8.10 (dd, *J* = 9.2, 2.8 Hz, 1H), 7.96 (dd, *J* = 8.7, 3.6 Hz, 1H), 7.93 (d, *J* = 8.8 Hz, 1H), 7.82 (d, *J* = 8.8 Hz, 1H), 7.79 (dd, *J* = 8.8, 3.9 Hz, 1H), 7.76 – 7.73 (m, 1H), 4.24 (d, *J* = 5.4 Hz, 1H), 4.12 (dd, *J* = 4.6, 2.6 Hz, 1H), 4.06 (dd, *J* = 4.6, 2.4 Hz, 1H), 4.03 (dd, *J* = 14.2, 7.1 Hz, 1H), 3.82 (s, 2H). HRMS (AP-ESI) m/z Calcd for $C_{19}H_{16}N_4O_8$ [M+H]+ 429.0968, found 429.1059.

General procedure for the preparation of 21a and its Analogue 21b-d.

Compounds 21a-d were synthesized by the same method as compound 16a-f.

5.1.17. 4-(2-(5'-chloro-2'-oxospiro[[1,3]dioxane-2,3'-indoline]-1'-yl)acetamido)-N-hydroxybenzamide (21a).

White solid, yield 34.2%. mp=133-134℃. ^{1}H NMR (600 MHz, DMSO) δ 11.13 (s, 1H), 10.71 (s, 1H), 10.22 (s, 1H), 7.90 (d, *J* = 8.7 Hz, 1H), 7.73 (d, *J* = 8.7 Hz, 1H), 7.70 (d, *J* = 8.8 Hz, 1H), 7.64 (d, *J* = 8.8 Hz, 1H), 7.47 – 7.42 (m, 2H), 7.07 – 7.05 (m, 1H), 4.72 (dt, *J* = 19.5, 9.8 Hz, 2H), 4.58 (d, *J* = 8.7 Hz, 2H), 3.96 (dd, *J* = 9.7, 5.2 Hz, 2H), 2.24 – 2.14 (m, 1H), 1.73 – 1.67 (m, 1H). HRMS (AP-ESI) m/z Calcd for $C_{20}H_{18}ClN_3O_6$ [M+H]+ 432.0884, found 432.0953.

5.1.18. 4-(2-(5'-chloro-2'-oxospiro[[1,3]dioxepane-2,3'-indoline]-1'-yl)acetamido)-N-hydroxybenzamide (21b).

White solid, yield 33.7%. mp=134-135℃. ^{1}H NMR (600 MHz, DMSO) δ 11.13 (s, 1H), 10.69 (s, 1H), 10.23 (s, 1H), 7.73 (s, 1H), 7.71 (dd, *J* = 4.7, 2.6 Hz, 2H), 7.70 – 7.68 (m, 1H), 7.63 (d, *J* = 8.8 Hz, 1H), 7.44 (dd, *J* = 8.4,

1.4 Hz, 1H), 7.07 (dd, *J* = 6.1, 2.3 Hz, 1H), 4.56 (s, 2H), 4.27 (d, *J* = 3.0 Hz, 2H), 4.03 (d, *J* = 4.3 Hz, 2H), 1.73 (d, *J* = 3.9 Hz, 4H). HRMS (AP-ESI) m/z Calcd for $C_{21}H_{20}ClN_3O_6$ [M+3H]+ 448.1041, found 448.1106.

5.1.19. 4-(2-(5'-bromo-2'-oxospiro[[1,3]dioxane-2,3'-indoline]-1'-yl)acetamido)-N-hydroxybenzamide (21c).

White solid, yield 40.3%. mp=142-143℃. ^{1}H NMR (600 MHz, DMSO) δ 11.12 (s, 1H), 10.75 (s, 1H), 10.66 (s, 1H), 7.90 (d, *J* = 8.7 Hz, 1H), 7.72 (d, *J* = 8.7 Hz, 1H), 7.69 (d, *J* = 8.8 Hz, 1H), 7.63 (d, *J* = 8.8 Hz, 1H), 7.52 (d, *J* = 2.2 Hz, 1H), 7.50 – 7.48 (m, 1H), 7.11 – 7.09 (m, 1H), 4.56 (d, *J* = 8.6 Hz, 2H), 4.34 (d, *J* = 6.5 Hz, 4H), 1.19 (dd, *J* = 28.9, 14.1 Hz, 2H).

5.1.20. 4-(2-(5'-bromo-2'-oxospiro[[1,3]dioxepane-2,3'-indoline]-1'-yl)acetamido)-N-hydroxybenzamide (21d).

White solid, yield 35.1%. mp=130-131℃. ^{1}H NMR (600 MHz, DMSO) δ 10.74 (s, 1H), 10.65 (s, 1H), 10.18 (s, 1H), 7.90 (d, *J* = 8.7 Hz, 1H), 7.81 (d, *J* = 2.0 Hz, 1H), 7.72 (d, *J* = 8.8 Hz, 1H), 7.69 – 7.67 (m, 1H), 7.63 (d, *J* = 8.8 Hz, 1H), 7.57 (dd, *J* = 8.4, 2.0 Hz, 1H), 7.05 – 7.01 (m, 1H), 4.56 (d, *J* = 8.7 Hz, 2H), 4.27 (d, *J* = 12.2 Hz, 2H), 4.04 – 4.01 (m, 2H), 1.73 (s, 4H). HRMS (AP-ESI) m/z Calcd for $C_{21}H_{20}ClN_3O_6$ [M+H]+ 492.0515, found 492.0614.

General procedure for the preparation of 25a and its Analogue 25b.

Compounds **23a-b** were synthesized by the same method as compound **14a**, and Compounds **25a-b** were synthesized by the same method as compound **16a**.

5.1.21. 4-(3-(5'-bromo-2'-oxospiro[[1,3]dioxane-2,3'-indoline]-1'-yl)propanamido)-N-hydroxybenzamide (25a).

White solid, yield 63.7%. mp=159-160℃. ^{1}H NMR (600 MHz, DMSO) δ 11.11 (s, 1H), 10.39 (s, 1H), 10.23 (s, 1H), 7.88 – 7.86 (d, *J* = 8.8 Hz, 1H),

7.71 – 7.66 (dd, *J* = 8.4, 20.4 Hz, 2H), 7.61 – 7.60 (m, 2H), 7.51 (s, 1H), 7.16– 7.14 (d, *J* = 7.8 Hz, 1H), 4.72– 4.68 (t, *J* = 9.6 Hz, 2H), 3.85– 3.82 (t, *J* = 7.2 Hz, 4H), 2.69– 2.67 (t, *J* = 7.2 Hz, 2H), 2.17– 2.15 (t, *J* = 7.2 Hz, 1H), 1.69– 1.66 (d, *J* =13.2 Hz, 1H). HRMS (AP-ESI) m/z Calcd for $C_{21}H_{20}BrN_3O_6$ [M+H]+ 490.0535, found 490.0611.

5.1.22. 4-(4-(5'-bromo-2'-oxospiro[[1,3]dioxane-2,3'-indoline]-1'-yl)butanamido) -N-hydroxybenzamide (25b).

White solid, yield 58.4%. mp=160-161℃. ^{1}H NMR (600 MHz, DMSO) δ11.09 (s, 1H), 10.15 (s, 1H), 10.11 (s, 1H), 7.70 – 7.68 (d, *J* = 8.4 Hz, 2H), 7.64 – 7.62 (d, *J* = 8.4 Hz, 3H), 7.53 (s, 1H), 7.13 – 7.12 (d, *J* = 7.8 Hz, 1H), 4.73– 4.70 (t, *J* = 10.2 Hz, 2H), 3.92 – 3.91 (d, *J* = 8.4 Hz, 2H), 3.69– 3.67 (t, *J* = 6.6 Hz, 2H), 2.43 – 2.39 (dd, *J* = 10.2, 15.6 Hz, 2H), 2.17– 2.15 (t, *J* = 6.6 Hz, 1H), 1.88– 1.85 (t, *J* = 13.8 Hz, 2H), 1.69 – 1.67 (d, *J* = 12.0 Hz, 1H). HRMS (AP-ESI) m/z Calcd for $C_{22}H_{22}BrN_3O_6$ [M+H]+ 504.0692, found 504.0759.

General procedure for the preparation of20c,26, and 27.

5.1.23. Methyl-4-(2-(5'-bromo-2'-oxospiro[[1,3]dioxane-2,3'-indoline]-1'-yl)aceta mido)benzoate (20c).

White solid, yield 80.1%. mp=234-235℃. ^{1}H NMR (600 MHz, DMSO) δ 10.75 (s, 1H), 7.93 (d, *J* = 8.8 Hz, 2H), 7.71 (d, *J* = 8.8 Hz, 2H), 7.58 (dd, *J* = 8.4, 2.1 Hz, 1H), 7.54 (d, *J* = 2.0 Hz, 1H), 7.03 (d, *J* = 8.4 Hz, 1H), 4.72 (dd, *J* = 11.8, 9.3 Hz, 2H), 4.57 (s, 2H), 3.98 – 3.93 (m, 2H), 3.82 (s, 3H), 2.23 – 2.15 (m, 1H), 1.69 (d, *J* = 13.5 Hz, 1H). HRMS (AP-ESI) m/z Calcd for $C_{21}H_{19}BrN_2O_6$ [M+H]+ 475.0426, found 475.0500.

5.1.24. 4-(2-(5'-bromo-2'-oxospiro[[1,3]dioxane-2,3'-indoline]-1'-yl)acetamido)b enzoic acid (26).

To a solution of KOH (0.3 g, 5.36 mmol) in 50 mL alcohol and 25 mL H_2O was added compound **20c** (1.43 g, 3.00 mmol). Keep the reaction for 1h at room temperature. The alcohol was removed in vacuum. Then 1N HCl

solution was added to the remaining mixture gradually until the solution became acidic and a white precipitate was generated. Concentrated the mixture and compound **26** was obtained as white solid (1.32 g, 95.5% yield), mp=202-203℃. ^{1}H NMR (600 MHz, DMSO) δ 12.69 (d, *J* = 69.0 Hz, 1H), 10.71 (s, 1H), 7.90 (d, *J* = 8.6 Hz, 2H), 7.68 (d, *J* = 8.6 Hz, 2H), 7.58 (dd, *J* = 8.4, 1.4 Hz, 1H), 7.54 (s, 1H), 7.02 (t, *J* = 8.4 Hz, 1H), 4.72 (t, *J* = 10.8 Hz, 2H), 4.57 (s, 2H), 3.98 – 3.92 (m, 2H), 2.23 – 2.16 (m, 1H), 1.70 (d, *J* = 13.4 Hz, 1H). HRMS (AP-ESI) m/z Calcd for $C_{20}H_{17}BrN_2O_6$ [M+H]+ 461.0270, found 461.0337.

5.1.25. N-(2-aminophenyl)-4-(2-(5'-bromo-2'-oxospiro[[1,3]dioxane-2,3'-indoline]-1'-yl)acetamido)benzamide (27).

Compound **26** (0.69 g, 1.5 mmol) was dissolved in 30 mL anhydrous THF. Then N-methylmorpholine (0.36mL, 3.3mmol) and isobutyl chloroformate (0.23mL, 1.8mmol) was added to this solution at -15℃ and stirred the mixture for 1h at the some temperature. Then o-phenylenediamine (0.18g, 1.65mmol) was added to the mixture and stirred for 1h at -15℃ and for another 12h at room temperature. Concentrated and removed the solvent with a rotary evaporator. The residue was dissolved in 50mL EtOAc and washed with brine (10mL×2). Then the organic phase was dried over anhydrous Na_2SO_4 and concentrated under low pressure to get the crude product. Finally, compound **27** was separated by column chromatography (P/E=2:1) as reddish brown solid (0.70 g, 84.6% yield), mp=228-229℃. ^{1}H NMR (600 MHz, DMSO) δ 10.67 (s, 1H), 9.59 (s, 1H), 7.97 (d, *J* = 8.2 Hz, 2H), 7.69 (d, *J* = 8.4 Hz, 2H), 7.62 – 7.57 (m, 1H), 7.55 (s, 1H), 7.15 (d, *J* = 7.6 Hz, 1H), 7.04 (d, *J* = 8.4 Hz, 1H), 6.96 (t, *J* = 7.5 Hz, 1H), 6.78 (d, *J* = 7.9 Hz, 1H), 6.59 (t, *J* = 7.4 Hz, 1H), 4.88 (s, 2H), 4.73 (t, *J* = 10.8 Hz, 2H), 4.58 (s, 2H), 3.96 (d, *J* = 7.5 Hz, 2H), 2.24 – 2.15 (m, 1H), 1.70 (d, *J* = 13.3 Hz, 1H). HRMS (AP-ESI) m/z Calcd for $C_{20}H_{17}BrN_2O_6$ [M+H]+ 551.0852, found 551.0924.

5.2. Biological evaluation

5.2.1. In vitro HDACs inhibition fluorescence assay.

The HDACs enzyme extracted from Hela nuclear was used in this testing procedure. First, 50μL of tested compound solution in a variety of concentrations was mixed with 10μL of HDACs enzyme solution. Five minutes later, 40μL Boc-Lys (acetyl)-AMC was added as fluorogenic substrate, and then the mixture was incubated for 30 min at 37 □. Finally,100μL Trypsin solution was added in order to stop the hydrolytic reaction. After incubation for another 20 min at 37□, the hydrolysate was monitored using a UV-vis spectrophotometer through the change in the absorbance measured at 390 nm and 460 nm.

5.2.2. In vitro antiproliferative assay.

All cell lines were grown in RPMI1640 medium with 10% FBS at 37□ in 5% CO_2 humidified incubator. First, cells were pated in 96-well plates (5000/well), and allowed to grow for at least 4 hours. Then different concentrations of compounds were added. The plates were put in the incubator to keep on cultivating for another 48 hours. Then 1% MTT (3-[4,5-dimethyl-2-thiazolyl]-2,5-diphenyl-2H-tetrazolium bromide) solution was added to each well. Four hours later, DMSO was added to dissolve formazan and mixed for 15 min. Finally, the optical density values were measured using a UV-vis spectrophotometer at 570nm.

5.2.3. In vivo antitumor assay against H7402 xenograft.

In order to investigate the in vivo antitumor capability, H7402 human hepatoma cells (6.88×10^7) were inoculated subcutaneously in the right axilla of each male athymic nude mouse (4-6 weeks old, Beijing HFK Bioscience Co. Ltd.). Eight days later, the average volume of all the tumors had grown to 140mm^3, and then nude mice were grouped randomly into treatment and control groups (seven mice per group). Treatment groups received 60mg/kg/d compound **25a** or 100mg/kg/d compound **SAHA** respectively, and blank control group received PBS solution in an equal volume. Since the day of

gavage administration, tumor volumes and body weight was measured every three days. Tumor volumes were measured using a vernier caliper through the equation ($V=ab^2/2$, where a and b represent the longest and shortest diameter, respectively). Relative increment ratio(T/C) was calculated based on the following formula:

T/C (%) = the treatment group (T) RTV/the blank control group (C) RTV

where RTV, named relative tumor volume $=V_t/V_0$ (V_t: the tumor volume measured at the end of treatment; V_0: the tumor volume measured at the beginning of grouping).

Acknowledgments

This work was supported by National Science and Technology Specific Projects of China (No. 2009ZX09103-118) and National Nature Science Foundation of China (Nos. 90713041 and 30772654) and National Natural Science Foundation of China (Grant No. 21172134).

References and notes

1. Zhang, Y.; Feng, J.; Jia, Y.; Wang, X.; Zhang, L.; Liu, C.; Fang, H.; Xu, W. *J Med Chem* **2011**, *54*, 2823.
2. Hassig, CA.; Schreiber, SL. *Curr Opin Chem Biol* **1997**, *1*, 300.
3. Tony, Kouzarides. *Current Opinion in Genetics & Development* **1999**, *9*, 40.
4. Wolffe, AP. *Science* **1996**, *272*, 371.
5. Glozak, MA.; Sengupta, N.; Zhang, X.; Seto, E. *Gene* **2005**, *363*, 15.
6. Choi, E.; Lee, C.; Park, JE.; Seo, JJ.; Cho, M.; Kang, JS.; Kim, HM.; Park, SK.; Lee, K.; Han, G. *Bioorganic & Medicinal Chemistry Letters* **2011**, *21*, 1218.
7. de Ruijter, AJ.; van Gennip, AH.; Caron, HN.; Kemp, S.; van Kuilenburg, AB. *Biochem J* **2003**, *370*, 737.
8. Halkidou, K.; Gaughan, L.; Cook, S.; Leung, HY.; Neal, DE.; Robson, CN. *Prostate* **2004**, *59*, 177.
9. Choi, JH.; Kwon, HJ.; Yoon, BI.; Kim, JH.; Han, SU.; Joo, HJ.; Kim, DY. *Jpn J Cancer Res* **2001**, *92,* 1300.
10. Wilson, AJ.; Byun, DS.; Popova, N.; Murray, LB.; L'Italien, K.; Sowa, Y.; Arango, D.; Velcich, A.; Augenlicht, LH.; Mariadason, JM. *J Biol Chem* **2006**, *281*, 13548.
11. Zhang, Z.; Yamashita, H.; Toyama, T.; Sugiura, H.; Ando, Y.; Mita, K.; Hamaguchi, M.; Hara, Y.; Kobayashi, S.; Iwase, H. *Breast Cancer Res Treat* **2005**, *94*, 11.
12. Zhu, P.; Martin, E.; Mengwasser, J.; Schlag, P.; Janssen, KP.; Göttlicher, M. *Cancer Cell* **2004**, *5*, 455.
13. Huang, BH.; Laban, M.; Leung, CH.; Lee, L.; Lee, CK.; Salto-Tellez, M.; Raju, GC.; Hooi, SC. *Cell Death Differ* **2005**, *12*, 395.
14. Song, J.; Noh, JH.; Lee, JH.; Eun, JW.; Ahn, YM.; Kim, SY.; Lee, SH.; Park, WS.; Yoo, NJ.; Lee, JY.; Nam, SW. *APMIS* **2005**, *113*, 264.
15. Zhang, Z.; Yamashita, H.; Toyama, T.; Sugiura, H.; Omoto, Y.; Ando, Y.; Mita, K.; Hamaguchi, M.; Hayashi, S.;, Iwase, H. *Clin Cancer Res* **2004**,

10 ,6962.
16. Grant, S.; Easley, C.; Kirkpatrick P. *Nat Rev Drug Discov* **2007**, *6*, 21.
17. Campas-Moya C. *Drugs Today (Barc)* **2009**, *45*, 787.
18. Kang, J.; Xiaopan, Z.; Chunhua, M.; Yingying, X.; Yumei, Yuan.; Wenfang, X. *Bioorg. Med. Chem* **2013**, *21*, 2663.

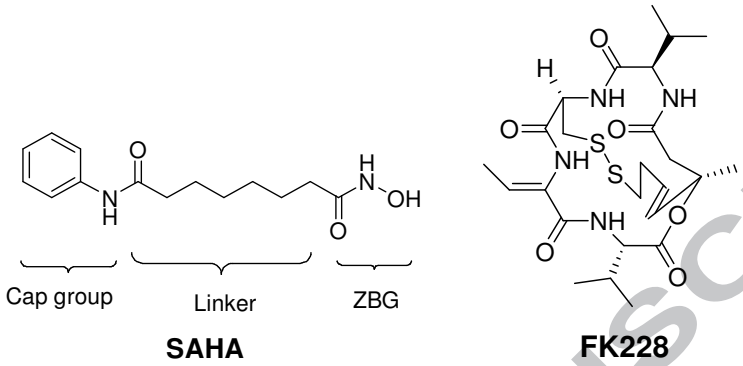

Figure 1. The structures of SAHA and FK228.

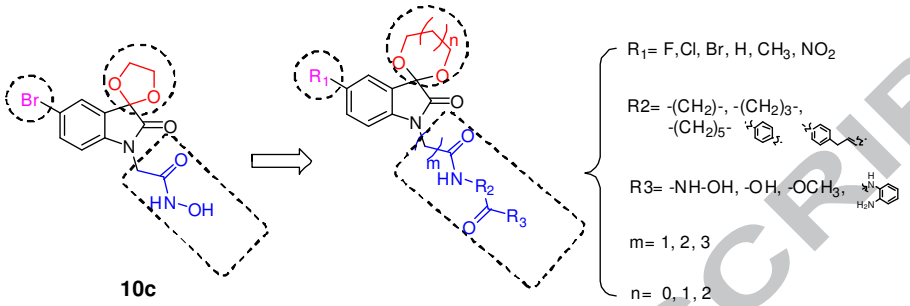

Figure 2. The new HDAC inhibitors derived from compound **10c**.

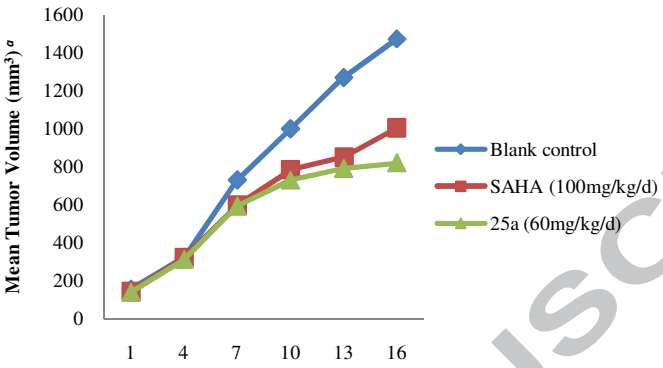

Figure 3. Antitumor activity of **25a** and **SAHA** against H7402 human tumor xenografts implanted in nude mice. The values are mean tumor volume in at least three experiments. [a] Values are the mean of three experiments. The standard derivations are <20% of the mean.

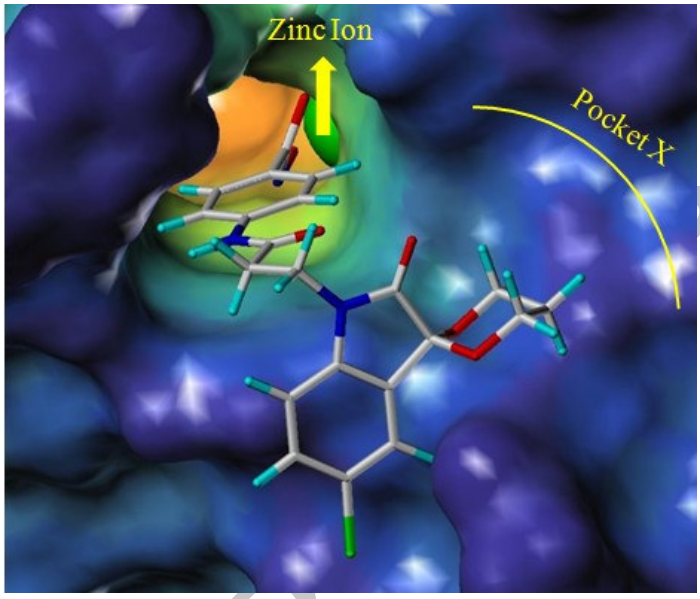

Figure 4. The FlexX docking result of **25a** with HDAC8 (PDB entry: 1T64).

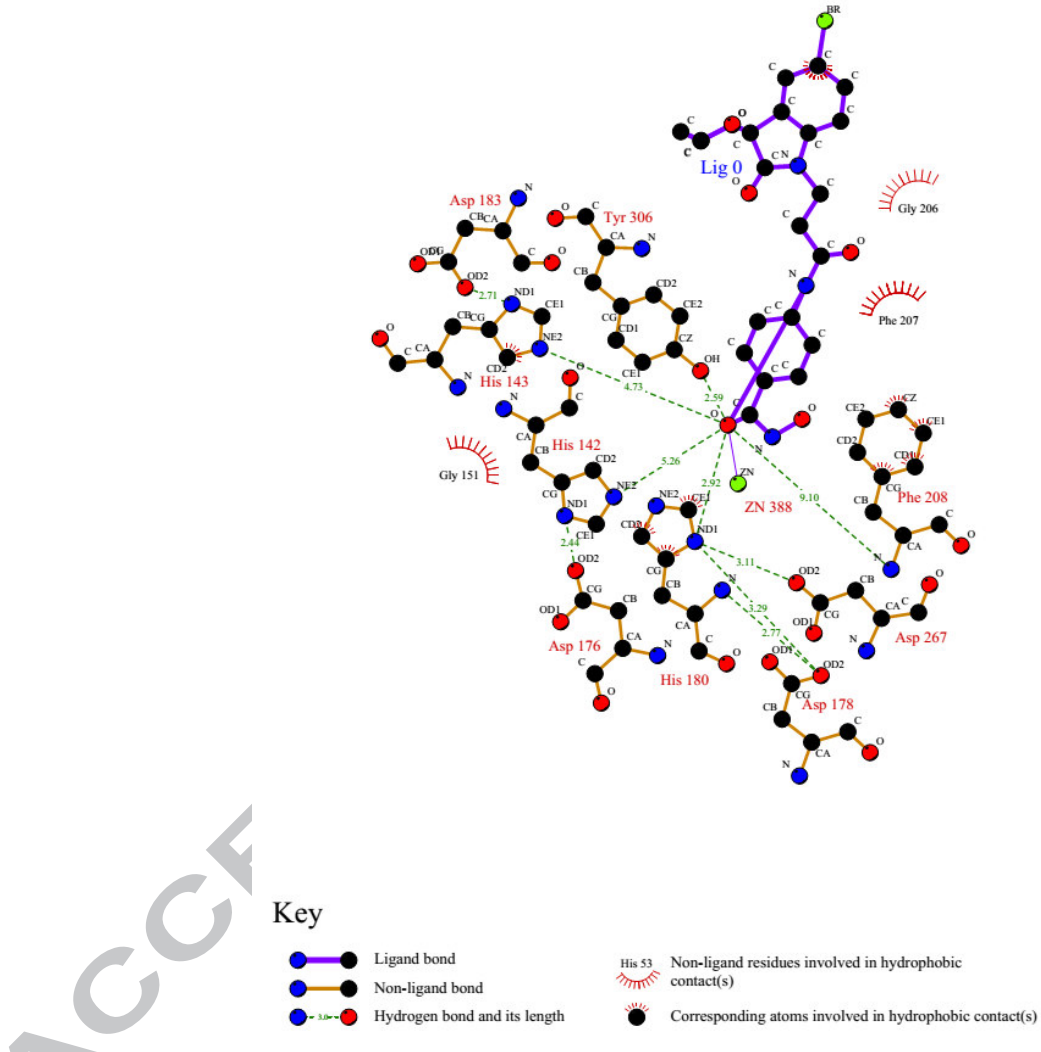

Figure 5. The docking result of **25a** shown by LIGPLOT.

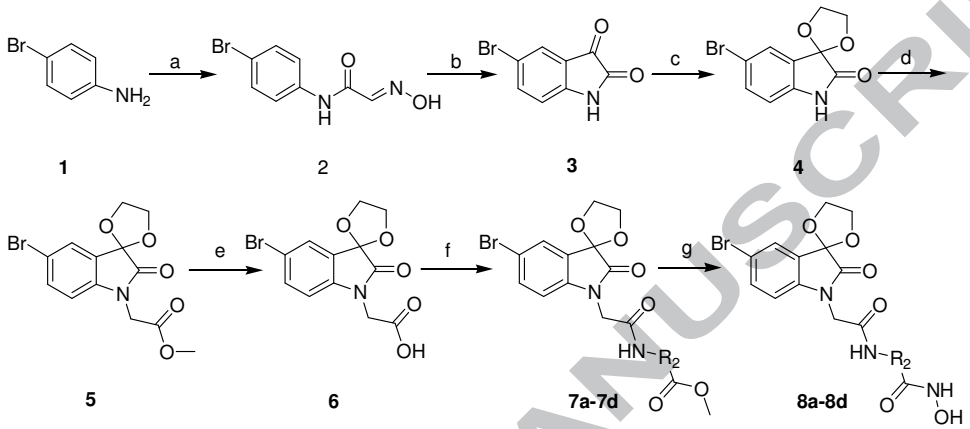

Scheme 1. (**1**)R_2= CH_2, $(CH_2)_3$, $(CH_2)_5$,  . (**2**)Reagents and conditions: (a) $Cl_3CH(OH)_2$, NH_2OH, Na_2SO_4, 85℃; (b) H_2SO_4, 90℃; (c) ethane-1,2-diol, TsOH, toluene, 130℃; (d) $BrCH_2COOCH_3$, TBAB, K_2CO_3, KI, acetone, 60℃; (e) EtOH, KOH, HCl; (f) amino acid methyl esters with different lengths, isobutyl chloroformate, NMM, THF, -20℃; (g) NH_2OK, CH_3OH.

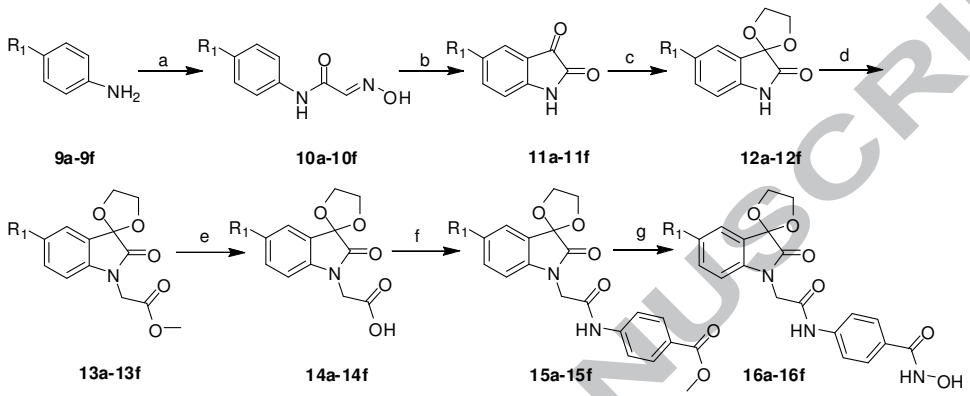

Scheme 2. (**1**)R_1= F, Cl, Br, H, CH_3, NO_2. (**2**)Reagents and conditions: (a) $Cl_3CH(OH)_2$, NH_2OH, Na_2SO_4, 85℃; (b) H_2SO_4, 90℃; (c) ethane-1,2-diol, TsOH, toluene, 130℃; (d) $BrCH_2COOCH_3$, TBAB, K_2CO_3, KI, acetone, 60℃; (e) EtOH, KOH, HCl; (f) methyl-4-aminobenzoate, isobutyl chloroformate, NMM, THF, -20℃; (g) NH_2OK, CH_3OH.

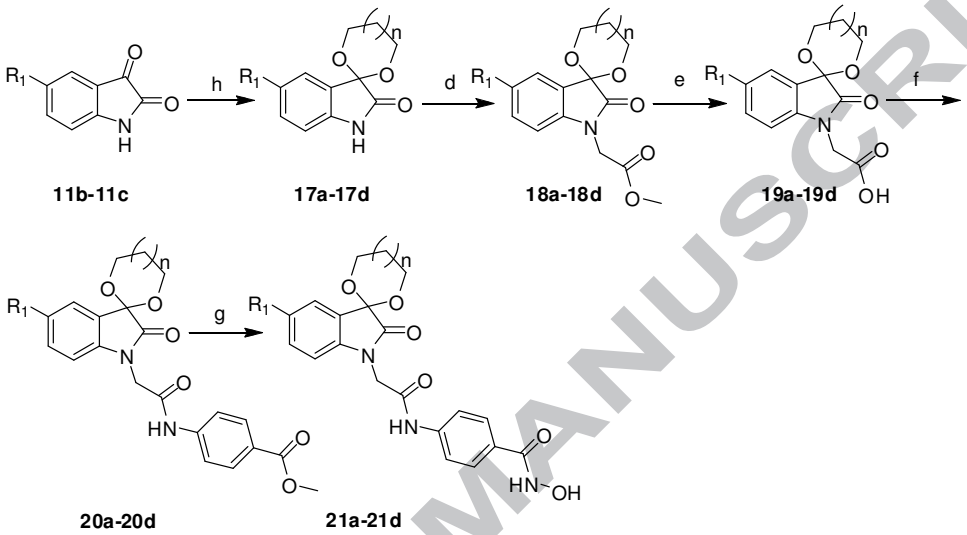

Scheme 3. (1) R_1= Cl or Br; n= 1 or 2. **(2)**Reagents and conditions: (h) propane-1,3-diol or butane-1,4-diol, TsOH, toluene, 130℃; (d) $BrCH_2COOCH_3$, TBAB, K_2CO_3, KI, acetone, 60 ℃ ; (e) EtOH, KOH, HCl; (f) methyl-4-aminobenzoate, isobutyl chloroformate, NMM, THF, -20℃; (g) NH_2OK, CH_3OH.

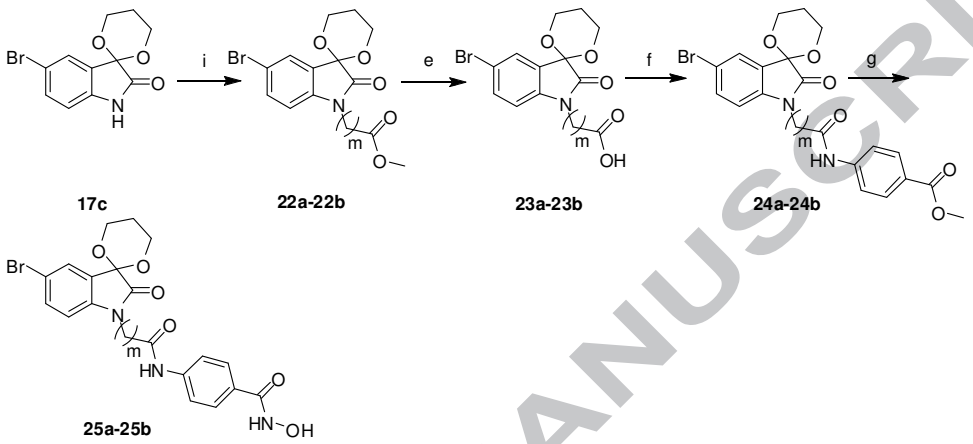

Scheme 4. (1)m= 2 or 3. (2)Reagents and conditions: (i) $BrCH_2CH_2COOCH_3$ or $Br(CH_2)_3COOCH_3$, TBAB, K_2CO_3, KI, acetone, 60℃; (e) EtOH, KOH, HCl; (f) methyl-4-aminobenzoate, isobutyl chloroformate, NMM, THF, -20℃; (g) NH_2OK, CH_3OH.

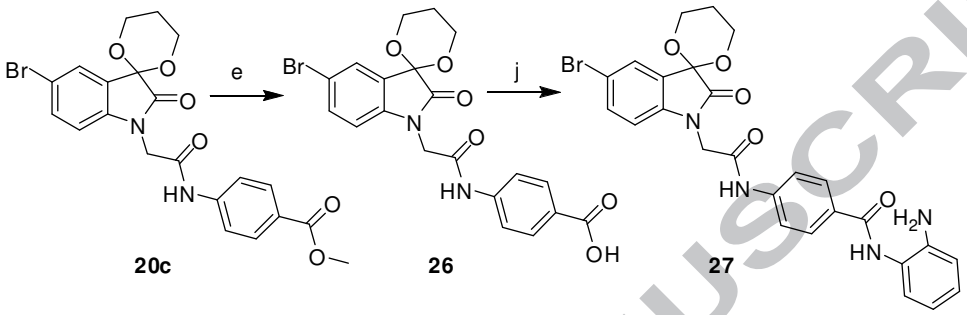

Scheme 5. Reagents and conditions: (e) EtOH, KOH, HCl; (j) benzene-1,2-diamine, isobutyl chloroformate, NMM, THF, -20℃.

Table 1.
HDACs Inhibition Activity of Compounds 8a-e, and SAHA

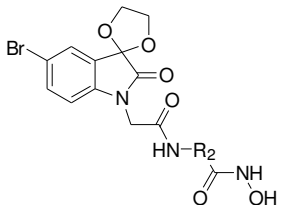

Compd	R_2	IC_{50} of HeLa nuclear extract (μmol) [a]
8a	**CH_2**	>50
8b	**$(CH_2)_3$**	0.92±0.023
8c	**$(CH_2)_5$**	0.67±0.011
8d		0.22±0.008
SAHA		0.11±0.014

[a]Results expressed as the mean ± standard deviation of at least three separate determinations.

Table 2.

HDACs Inhibition Activity of Compounds 16a-f, and SAHA

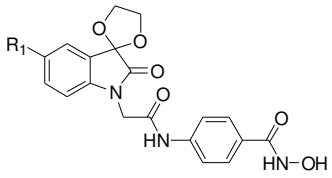

Compd	R_1	IC_{50} of HeLa nuclear extract (μmol) [a]
16a	**F**	0.19±0.012
16b	**Cl**	0.37±0.021
16c	**Br**	0.12±0.009
16d	**H**	0.31±0.031
16e	**CH_3**	0.28±0.022
16f	**NO_2**	>50
SAHA		0.11±0.014

[a] Results expressed as the mean ± standard deviation of at least three separate determinations.

Table 3.
HDACs Inhibition Activity of Compounds 21a-d, and SAHA

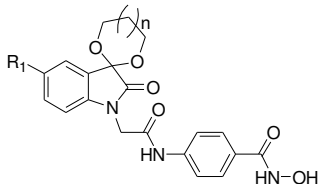

Compd	R_1	n	IC_{50} of HeLa nuclear extract (nmol) [a]
21a	**Cl**	**1**	34.4±2.74
21b	**Cl**	**2**	37.3±1.26
21c	**Br**	**1**	13.0±1.05
21d	**Br**	**2**	21.6±2.11
SAHA			0.11±0.014μmol

[a] Results expressed as the mean ± standard deviation of at least three separate determinations.

Table 4.

HDACs Inhibition Activity of Compounds 25a-b, and SAHA

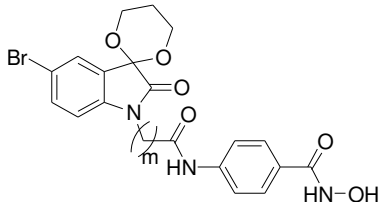

Compd	m	IC_{50} of HeLa nuclear extract (nmol) [a]
25a	**2**	10.13±1.18
25b	**3**	19.40±1.34
SAHA		0.11±0.014μmol

[a] Results expressed as the mean ± standard deviation of at least three separate determinations.

Table 5.

HDACs Inhibition Activity of Compounds 20c, 26, 27, and SAHA

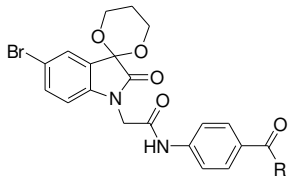

Compd	R	IC_{50} of HeLa nuclear extract (μmol) [a]
20c		>50
26		>50
27		0.31±0.027
SAHA		0.11±0.014

[a] Results expressed as the mean ± standard deviation of at least three separate determinations.

Table 6.

The anti-proliferative activities of compounds 21a-d, 25a-b,27, and SAHA against several representative tumor cell lines.

Compd	IC_{50} (μmol) [a]											
	PC-3	MDA-MB -231	K562	U937	H7402	MCF-7	Hela	HEL	KG1	ES-2	HCT116	3AO
21a	21.87	57.08	5.32	2.09	4.64	28.40	11.34	1.25	9.19	10.08	41.87	12.29
21b	11.56	36.38	7.23	1.49	5.34	25.02	36.05	1.29	10.05	25.26	42.42	23.55
21c	11.01	44.67	1.94	0.40	1.37	8.58	12.05	0.56	5.40	16.11	60.05	18.27
21d	17.68	24.11	3.91	0.66	0.75	6.13	>50	0.64	5.49	3.60	80.24	27.22
25a	1.91	100.84	0.18	0.14	5.33	52.65	2.79	0.33	0.32	2.80	1.26	3.25
25b	7.93	126.42	0.39	0.22	0.58	13.68	22.19	0.34	042	6.02	1.10	21.41
27	4.43	82.74	0.44	1.08	1.95	5.23	26.55	2.26	5.92	6.49	0.64	9.71
SAHA	1.92	13.48	1.44	0.37	10.11	0.58	5.45	1.74	0.64	3.46	0.33	79.30

[a] Values are the mean of three experiments. The standard derivations are <20% of the mean.

Table 7.
HDACs Inhibition Activity and Isoform Selectivity of Compounds 25a and SAHA

compd	IC_{50} of HeLa nuclear extract (nmol) [a]	IC_{50} of HDAC1 (nmol)[a]	IC_{50} of HDAC3 (nmol) [a]	IC_{50} of HDAC6 (nmol) [a]	HDAC3/HDAC1 isoform selectivity	HDAC3/HDAC6 isoform selectivity
25a	10.13	201.16	25.01	126.48	0.12	0.20
SAHA	110.23	203.06	52.99	202.11	0.26	0.26

[a] Values are the mean of three experiments. The standard derivations are <20% of the mean.

Graphical Abstract：

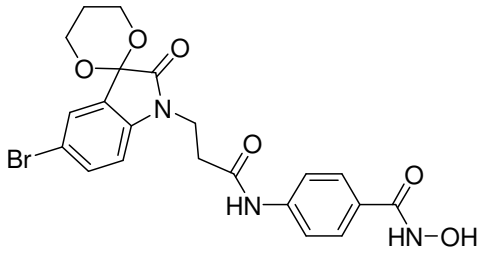

25a

(IC_{50}= 10.13 nM)